MODELING INCLUSIONS IN DEEP FOUNDATIONS INTEGRITY TESTED BY THERMAL METHODS

Matthew Baudo, Pile Dynamics, Inc., Solon, OH, USA, (216) 831-6131, mbaudo@pile.com
Brent Robinson, PhD, PE, Pile Dynamics, Inc., Solon, OH, USA, brobinson@pile.com

ABSTRACT

Circular and rectangular deep foundation elements are commonly tested by thermal integrity methods. A multiphysics model was adapted using COMSOL to evaluate the effect on thermal measurements of the size and extent of soil and weak concrete inclusions. The temperature changes as measured by nearby wires for small intrusions into the reinforcement cage at and between thermal measurement locations, exposed reinforcement and full cross section contamination are modeled. The modeled temperature versus depth results are analyzed directly as temperature versus depth profiles and a comparison to field measurements is also included. Detection limits and signatures of anomalies including soil inclusions on the shaft's edge, full cross section joints, and partial loss of reinforcement cage cover are modeled and described.

Keywords: Drilled Shafts, Numerical Models, Integrity Testing, Quality Assurance

INTRODUCTION

Integrity testing of deep foundation elements by thermal methods have been described in some detail over the past several years. As described by Mullins (2010), the method uses measurements of temperature versus depth, evenly distributed around the reinforcement cage or as a single wire on a center bar for smaller circular elements, to characterize the distribution and dissipation of heat generated by hydrating concrete. Regions cooler than the average are often indicative of areas of contaminated concrete or soil inclusions, while regions warmer than average are often indicative of zones of larger cross section or increased cement content. When coupled with the volume of concrete placed in the excavation, the thermal measurements have been used to estimate a profile of effective radius versus depth, and as an estimate of how well the cage is centered in the shaft's cross section.

Piscsalko et al. (2016) proposed a criteria to flag shafts tested by thermal methods for further evaluation. A proposed percentage reduction of the effective radius calculated from the concrete volume analysis would be applied in a way similar to those suggested by Sellountou et al. (2019) for crosshole sonic logging. There is demand for these types of more fixed criteria, particularly by owners who prefer to publish them in specifications or guidance documents.

Further examples detailing interpretation of case studies of the measured temperature versus depth plots and the effective radius analyses were described by Belardo et al (2021). They described the thermal and effective radius profiles for issues at the pile top, changes due to known environmental conditions, and profiles of cage shifting, local inclusions, inclusions that cover the entire cross section and bulges overlying reductions caused by cage removal. Coleman and Belardo (2023) provided several case studies reviewing interpretation inclusions at the shaft base.

From the outset, Mullins (2010) noted that these qualitative analyses of temperature versus depth and analyses supported by other field inspection could also be supplemented with more comprehensive numerical modeling. That modeling required much more detailed knowledge, especially of the physical and chemical make-up of the components for concrete mix design, the planned and as-built pile geometry and the soils and rock encountered during drilling.

PRIOR WORK

Johnson (2016) described a basis to numerically modelling circular drilled foundation in COMSOL Multiphysics®, a finite element software suite that solves coupled systems of partial differential equations (COMSOL, Inc., 2024). Concrete hydration is modeled by an Arrhenius model that includes equivalent age and degree of hydration, parameters for which have also been separately investigated and calibrated for a number of concrete mix designs by, for example Schindler and Folliard (2005). The hydrating concrete generates heat, which in turn is transferred to the surrounding modeled soil by the general heat equation. At the top of foundation element, a general heat flux surface simulates dissipation of heat in air. Table 1 describes the modelling parameters used to generate the model in this study. The hydration model parameters use mix number 10 from Schindler and Folliard, which included 70% Type I Portland cement and 30% ground-granulated blast furnace slag. This mix was selected as many of the concrete mixes encountered in the authors' experience includes some percentage of alternative cementitious material, and it yielded a peak temperatures in these models that were consistent with those observed on many sites for the modeled diameter.

Table 1. Modeling Parameters input into COMSOL for heat generation and transfer, after Schindler and Folliard (2005)

Concrete Hydration Model Parameters		**Saturated Sand Model Parameters**	
E, Activation Energy	51,510 J/mol	Thermal Conductivity	3 W/(m-K)
Beta, Hydration Shape Parameter	0.625	Density	1700 kg/m*3*
Tau, Hydration Time Parameter	25.22 hours	Heat Capacity	800 J/kg/K
Au, Ultimate degree of Hydration	0.822		
Hu, Heat of hydration of cementitious materials at 100% hydration	472 J/kg		
Initial Temperature	73 Deg F	Initial Temperature	73 Deg F
Wc, Weight of cement materials	614 kg/m*3*		
Ww, Weight of water	267 kg/m*3*		
Wca, Weight of course aggregate	802 kg/m*3*	Initial Air Temperature	73 Deg F
Wfa, Weight of fine aggregate	547 kg/m*3*		
Cc, Specific heat of cement	1000 J/kg/K		
Cw, Specific heat of water	4186 J/kg/K		
Cca, Specific heat of course aggregate	860 J/kg/K		
Cfa, Specific heat of fine aggregate	800 J/kg/K		

Amir and Amir (2022) similarly report on proprietary software developed to model a deep foundation element surrounded by soil, air or water. This report includes several scenarios for inclusions or loss of concrete cover modeling a reported 1.5 m diameter pile with thermal measurements in four locations.

CURRENT STUDY—MODELING WITH COMSOL

The models reviewed in this study start with a 1.5 m diameter circular drilled shaft, 10 m long. The shaft is bounded by saturated sands from the ground surface to 13 m and extending radially to 2.25 m from the center of the shaft to minimize boundary condition effects over the modeled time. The model was run to 100 hours, but the mix tended to peak at around 24 hours per the hydration parameters and shaft geometry. A series of inclusions were also modeled, indicating different common construction anomalies.

DOI:10.37308/DFI49.2024850111

Following ASTM D7949-14 (ASTM, 2014), the number of thermal measurement locations were spaced equally around the perimeter of the reinforcement cage location. The ASTM standard states “the location plan shall provide in most cases one access duct for every 300 mm of diameter, with a preferred minimum of four access ducts for elements with diameters 1 m or larger.” Thus, following the standard and standard of practice, 1.5 m divided by 0.3 m implies at least five measurement locations, spaced 72 degrees apart. Similarly, measurements of temperature specified by the standard require accuracy with 1 degree Celsius and readability to 0.1 degrees C, although sensors available for these measurements are often more sensitive.

The results of the COMSOL model allow for continuous temperature profiles with depth at any location and time in the pile. Thermal measurements are obtained by wires with discrete 300 mm spacing of the digital temperature sensors. These modeled data points are presented on a modelled “cut line” for reference. The cut-lines present data in-between the measured spaced points for reference. Different spacings between the sensors would be indicated by different data point locations on the same cut line.

For this paper, a circular foundation is modeled with the following inclusions:

1. A full cross-sectional inclusion of varying thicknesses, modeling a cold joint (albeit without a significant pause in time modeled between the sections of concrete above and below) or a temporary breach in a tremie.
2. A zone of exposed reinforcement, 1 m tall and varying the angle of lost cover.
3. A spherical soil inclusion from the outside to the inside, at two locations—one centered on a sensor location and one centered between four sensors.

Full cross section soil inclusion

A 3-D model was developed for sand inclusions, shown in Fig. 2. The COMSOL model, minus the inclusion, was the general basis for all three scenarios, as is the five wire layout shown in plan view. The thickness of the inclusion, t, was varied and presented here as 25, 75 and 150 mm. From a cross sectional area perspective, this inclusion is 100% of the cross section.

As shown in Fig. 3 and as expected, thicker layers yield larger reductions in temperature and larger vertical zones of influence. The thicker, 150 mm included layer shows temperature reductions from 4.2 to 5.7 m, while the thin 25 mm included layer shows temperature reductions between 4.5 to 5.4 m. Similarly, the temperature reduction at 25 mm is much smaller (1 degrees C) and therefore more subtle than the reduction at 150 mm (7.8 degrees C). The less severe inclusion will, therefore, be harder to identify. However, inspection of the temperature versus depth graphs in Fig. 2 clearly indicate the signature of the inclusion at temperature changes detectable by the sensors required by ASTM D7949. It should also be noted that, for different concrete mixes, the *absolute* value of temperature reduction will change, but the temperature reduction *relative* to the zones without such an inclusion will still be similar. Thermal methods look for changes in temperature, and whether those changes can be explained by planned geometries or environmental conditions or something outside the planned construction.

Other integrity methods, such as low strain testing or crosshole sonic logging would fair differently at the 25 mm thickness. A full layer reduction should fully interrupt the stress wave propagating down the pile for low strain testing, and a consequently “short” pile would be indicated. Crosshole sonic logging would also find most full layer inclusions, but the 25 mm thickness would depend strongly on how parallel the sensor probes are and their sampling. ASTM D6760 requires a minimum of 50 mm spacing between saved samples, at which this thin inclusion could be missed if the probes are parallel, and a sample is taken just above and just below the 25 mm inclusion.

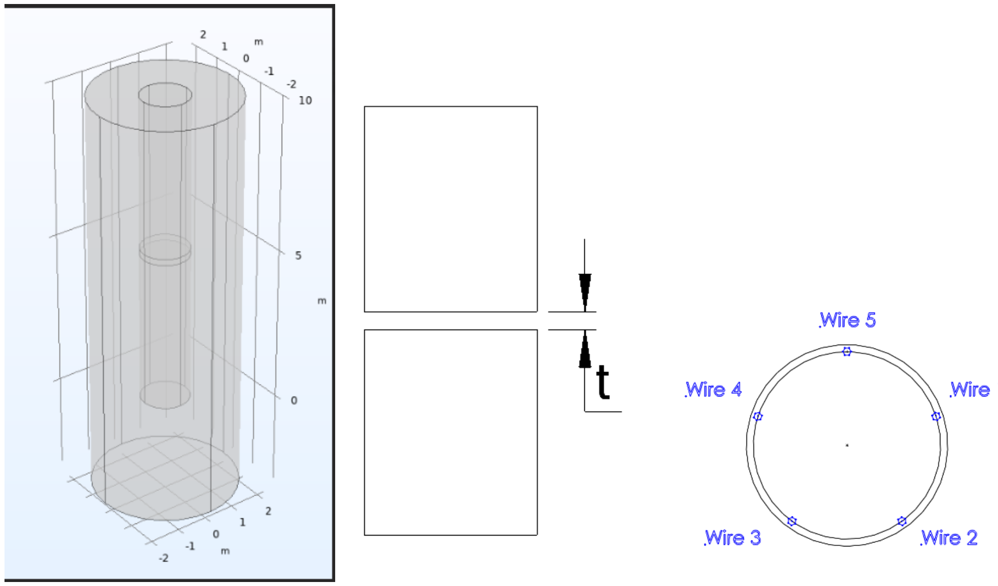

Fig. 2. COMSOL model, plan view of the variable inclusion thickness, and wire layout.

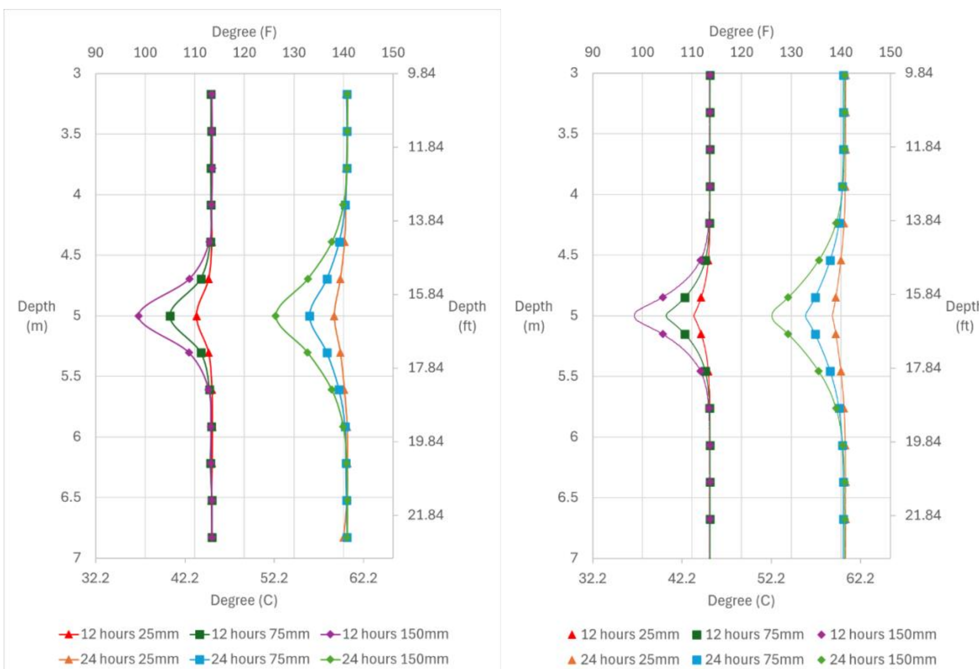

Fig. 3. Modeling results for all wires for the sand inclusion. A sensor (data point) is centered in the inclusion on the left, with sensors furthest from the inclusion and spaced 300 mm on the right.

Zone of exposed reinforcement

A zone reinforcement exposed to surrounding soil was modeled to review the expected temperature versus depth profile for a variety of portions of the perimeter, expressed in degrees. The loss is centered between two measurement locations, which are 72 degrees apart. Figure 4 shows the plan and isometric views of this cover loss. As the angle grows beyond 80 degrees, additional wires 3 and 5 would start to see temperature reductions as well. Presented in Fig. 5 are 20 degree and 80 degree cover losses, which correspond to 1% and 4% of the overall cross sectional area and shows this type of inclusion is much more likely to be of concern to those designing for durability than axial compression.

Again, the vertical zone of influence for the larger modeled cover loss in Fig. 5 stretches from 4.2 to 5.7 m, or just beyond the boundaries from 4.5 to 5.5 m. Temperature reductions are just above 3 degrees Celsius. As smaller cover loss zone centered between measurement points is indeed harder to find, a small 0.5 degree Celsius temperature reduction. It should be noted that if the smaller reduction was centered on a wire, the reduction in temperature would be large and seen only on that particular wire.

Other integrity methods would not find these inclusions. Low strain testing typically cannot find cross sectional area or impedance reductions of less than 20%. Crosshole sonic logging also does not currently find reductions outside of the reinforcement cage—the inclusion must interrupt and delay the wave between two access tubes.

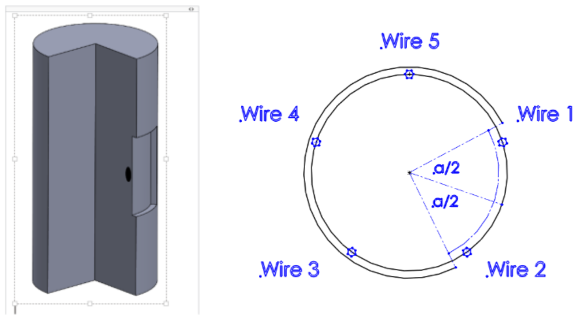

Fig. 4. Isometric and Plan views of the 1 m long vertical loss of concrete cover, with an angle, a.

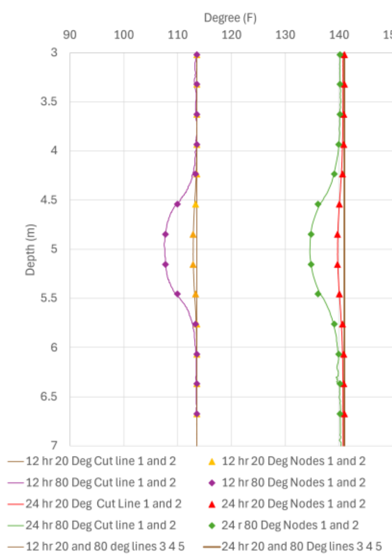

Fig. 5. Model temperature profiles for angles of 20 degree and 80 degree cover loss.

Soil inclusion

The final inclusions modeled are spheres of varying diameter, centered on the edge of the concrete, and creating radial inclusions into the pile. Two scenarios are investigated—one inclusion centered on the pile perimeter in line radially with a measurement location (the biggest expected change) and one centered on the pile perimeter between four measurement locations (the smallest expected change). The smallest

DOI:10.37308/DFI49.2024850111

radius presented in Fig. 7 is 200 mm, and the largest 500 mm. At the point of maximum cross sectional loss, this corresponds to reductions of 4% and 20% of the cross section, respectively.

When the inclusion is centered nearest a node location, Fig. 7, right indicates temperature reductions of 3 to 15 degrees C for inclusion radius of 200 and 500 mm. Also as expected, the vertical zone of influence grows as the radius increases, both at peak temperature of 24 hours, and at a time halfway to peak. When the inclusion is centered on the perimeter between four measurement locations (Fig. 7, left), the vertical extent of the temperature reductions is similar, but the maximum reduction is lower at 11 degrees C. However, the key difference in interpreting the extent of the two scenarios: the temperature reduction only occurs on wire 1 when centered on the wire, but the smaller temperature occurs on both wires 1 and 2 when centered between four sensors. As Mullins (2010) and others have previously described, determining the extent and location of an anomaly requires the analysis to look at not only temperature reduction, but the number of wires affected.

Other integrity methods would likely find some of these modeled inclusions. Low strain testing typically cannot find cross sectional area or impedance reductions of less than 20%, and therefore would likely register a small reflection for the 500 mm radial inclusion, regardless of its location. Crosshole sonic logging would certainly detect the inclusion of any size centered on measurement location 1, in profiles including tube 1. The profile between locations 2 and 5 would not register any of the three radii, and therefore the method would be unable to distinguish between the different radii. Crosshole sonic logging would also detect the 500 mm radius inclusion centered between the tubes. The inclusion would include measurement locations 1 and 2, and would reduce or interrupt the signal for all profiles including those two access ducts. The travel time would not be interrupted between measurement locations 1 and 2 for the 200 or 250 mm radius inclusion, and thus unlikely to be detected by FAT or energy criteria for CSL.

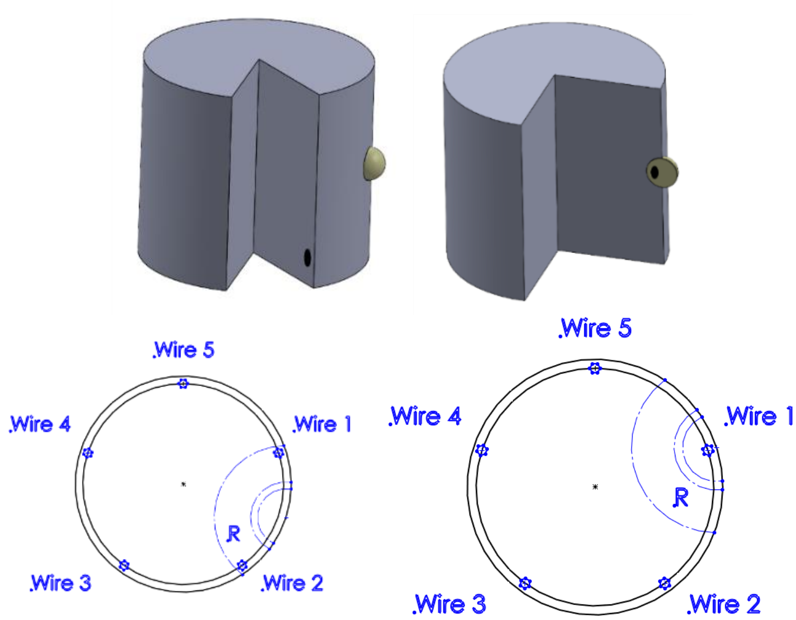

Fig. 6. Isometric and Plan views of a spherical soil inclusion centered between four measurement points (left) and centered on a measurement location (right). The three circles in the inclusion are to scale, with radii of 200, 250 and 500 mm.

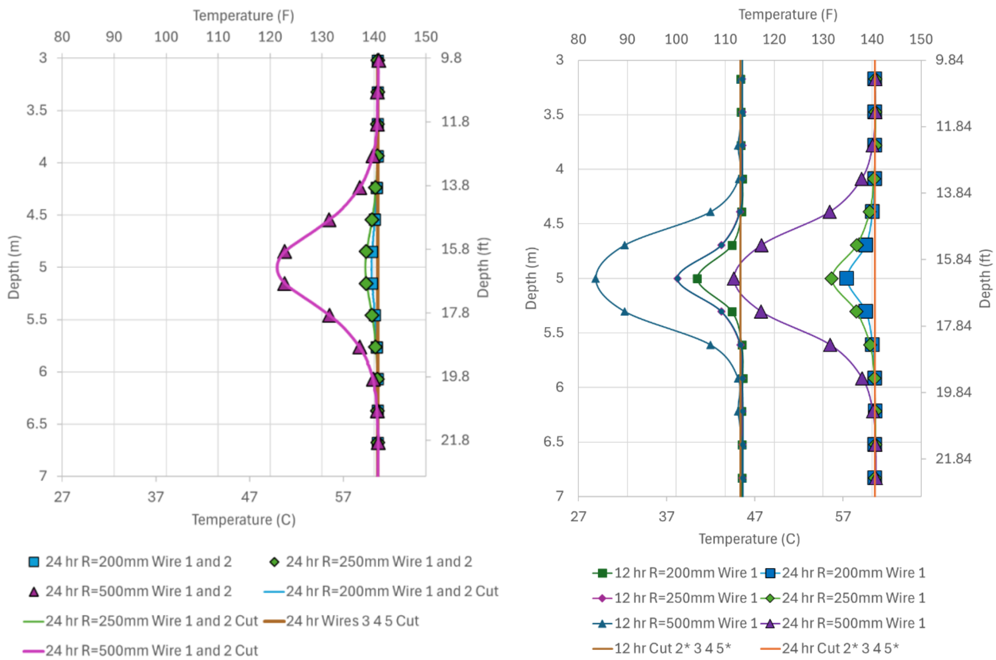

Fig. 7. Temperature versus depth profiles for 200 mm, 250 mm, and 500 mm radius inclusions. *-For the 500 mm radius inclusion centered on measurement location 1, locations 2 and 5 also indicate small temperature reductions of approximately 1 degree Celsius.

COMPARING TO FIELD MEASUREMENTS

For comparison, field data from a research project detailed in Stark et al. (2022) with intentionally installed anomalies were reviewed. Shaft 3 was built with a 1.22 m (48 inch) diameter temporary casing to 8 m (26 ft). From this depth to 13 m (42.5 ft), a 1.07 m (42 inch) diameter auger was used through silty clay and 1.37 m (4.5 ft) of limestone. The cage diameter (914 mm, 36 inch) was constant over the entire length. Intentional defects installed included tremie pipe lifts at approximately 3.7 m (12 ft) and 8.5 m (28 ft). An approximately 150 mm (6 inch) thick soil inclusion of rock cuttings were added at the base.

Reviewing the temperature versus depth curves reproduced in Fig. 8, the researchers and consultants identified localized temperature reductions in all measurement locations for Shaft 3 at 8.5 to 9.4 m (28 to 31 feet). Two of four measurement locations, 1 and 2, also identified smaller reductions in temperature at 2.7 to 3 m (9 to 10 feet). This corresponded to the approximate depth of the tremie pipe lifts. The vertical extent of the temperature reduction in the lower tremie lift is approximately 0.9 m (3 ft), while the upper tremie lift has much more limited vertical extent. Coring near the center did not indicate a joint in the upper lift, but did confirm the lower tremie lift. Coring nearest wire 2 indicated a small joint at 3.5 m (11.5 ft) and similarly confirmed the lower tremie lift.

A model of the shaft in COMSOL was built with sand layers of thickness 12 mm (0.5 in) at 3.7 m (12 ft) and 125 mm (5 in) centered at 9 m (30 ft). Modeled thicknesses were chosen based on the field temperature and coring measurements. The diameter reduction was modeled at 8 m, and the properties in Table 1 were carried over into this model. To match the maximum average temperature measured in the upper 8 m, the air temperature was reduced to 2^{o}C (35^{o}F) to match the above ground temperature indicated in Fig. 8, while the initial soil and air temperature was reduced to 15.5 ^{o}C (60^{o}F). The four wire locations were modeled on a centered cage, and the plots in Fig. 8 were shifted by tenths of degrees such that they were slightly separated. No effort was made in this paper to account for the eccentricity of the cage indicated by the measured curves, as it is outside this study's scope.

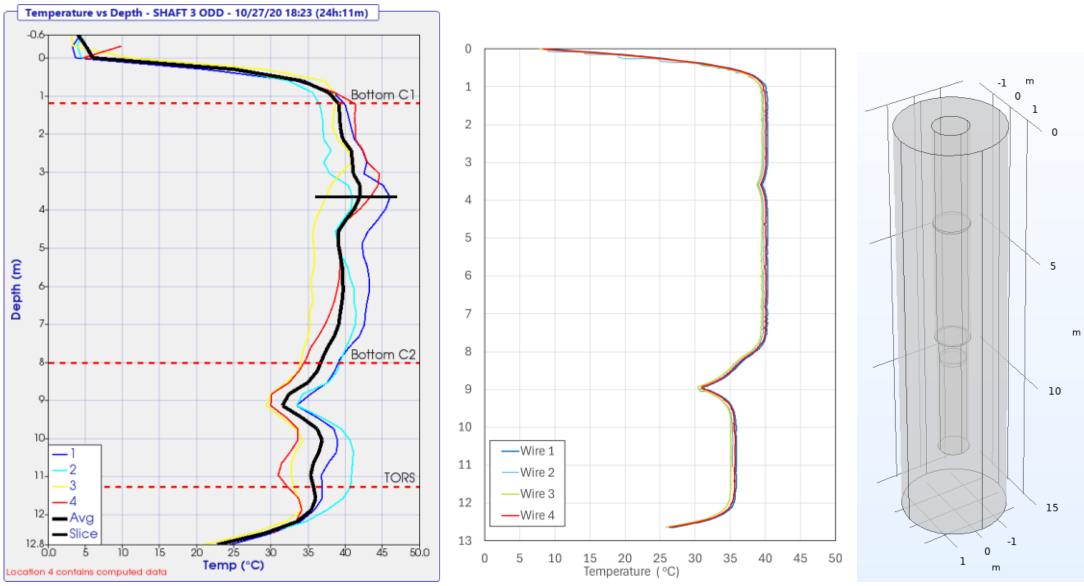

Fig. 8. Odd Wires from Drilled Shaft 3 Case History Measured at Peak Temperature, Figure 139, Stark et al. (2022), Reprocessed in SI Units (left); COMSOL Model and Results for Centered Cage (center, right)

The modeling results in Fig. 8 indicate crisper transitions from the assumed, stepped diameter change at 8 m (26 ft) than observed in the measurements, and the thickness of the inclusion modeled to simulate the tremie lift has a similar temperature reduction but a sharper, shorter vertical extent than the measurement. The smaller temperature reduction from the smaller inclusion from the short tremie lift modeled at 3.5 m (11.5 feet) was observed in wires 1 and 2, and may be more similar to the local inclusions of Figs. 6 and 7 than the full layer inclusion assumed. That is partly supported by the cores, which found nothing in the center but a zone of contaminated concrete in the core on the east side of the shaft. The rock and soil cuttings at the base of the shaft started at the location of the very last node (12.8 m, or 42 ft). This likely hindered detection of the soft bottom. Further modeling could also attempt to better match the oversized section near a ground water table between 2 and 3 m, as well as the previously discussed cage eccentricities.

CONCLUSIONS

Numerical modeling is an additional tool to probe the limits of detection when integrity testing deep foundations using thermal methods for a variety of soil inclusions, layers of weaker or stronger concrete, changes in curing environment or pile geometry. A small study of reductions of 20% or less of the cross section has indicated the shape of the temperature versus depth curve, and indicated relative reductions in temperature for a very specific modeled concrete mix. The field measurements and coring of a shaft with intentional tremie lifts matches well with model developed from the project's as-built drawings, with relatively few changes required to the assumed concrete hydration parameters. The numerical study's cross sectional reductions of less than approximately 5% provide faint signals at best, as do both the numerical and field study's full layer defects with thicknesses of less than 50 mm (2 inches). This is more sensitive or in line with other integrity methods commonly applied to deep foundation elements, and the profession must come to terms with what level of reduction is acceptable to maintain the expected performance of the deep foundation element.

REFERENCES

ASTM D7949-14 Standard Test Methods for Thermal Integrity Profiling of Concrete Deep Foundations, ASTM International, West Conshohocken, PA, 2014.

ASTM D6760-16 Standard Test Method for Integrity Testing of Concrete Deep Foundations by Ultrasonic Crosshole Testing, ASTM International, West Conshohocken, PA, 2016.

Amir, E. I., & Amir, J. M. (2022, September 20). Flaw detection threshold of thermal integrity testing. 11th International Conference on Stress Wave Theory and Design and Testing Methods for Deep Foundations, Rotterdam, The Netherlands.

Belardo, D., Robertson, S. and Coleman, T. "Interpretation and Evaluation of Thermal Integrity Profiling Measurements. Proceedings of the DFI Annual Conference (2021).

Coleman, T., Belardo, D. (2023). Drilled Shaft Base Quality Reductions Identified with Thermal Integrity Profiling. Presented at DFI 48th Annual Conference; 2023

COMSOL, Inc. (2024). COMSOL Multiphysics version 6.2 https://www.comsol.com/

Johnson, K. Thermal Integrity Analysis of Concrete Bridge Foundations Using COMSOL Multiphysics® Software, Proceedings of the 2017 COMSOL Conference, (2017).

Mullins, G. "Thermal Integrity Profiler of Drilled Shafts." DFI Journal, Vol. 4, No. 2, Deep Foundations Institute, (2010)

Piscsalko, G, Likins, G. and Mullins, G. (2016): Drilled shaft acceptance criteria based upon thermal integrity profiling. DFI 41st DFI Annual Conference on Deep Foundation, New York, New York, October

Schindler, A.K. and Folliard, K.J. (2005). "Heat of Hydration Models for Cementitious Materials" ACI Materials Journal, V. 102, No. 1 (2005).

Sellountou, A., Amir, J., Canivan, G., Chernauskas, L., Hertlein, B., Kandaris, P., Kovacs, T. and Likins, G. (2019): Terminology and Evaluation Criteria of Crosshole Sonic Logging (CSL) as applied to Deep Foundations*. Deep Foundations Institute

Stark, T.D., Idries, A, and Osouli, A. (2022). "Evaluating the Accuracy and Use of Drilled Shaft Integrity Testing Methods in Illinois", Illinois Department of Transportation, Bureau of Research.